JMolMed

ORIGINAL ARTICLE

Endoplasmic reticulum stress induces hepatic steatosis through interaction between PPARα and FoxO6 in vivo and in vitro

Dae Hyun Kim[1]

Abstract

Endoplasmic reticulum (ER) stress is a major cause of hepatic steatosis through increasing de novo lipogenesis. Forkhead box O6 (FoxO6) is a transcription factor mediating insulin signaling to glucose and lipid metabolism. Therefore, dysregulated FoxO6 is involved in hepatic lipogenesis. This study elucidated the role of FoxO6 in ER stress–induced hepatic steatosis in vivo and in vitro. Hepatic ER stress responses and β-oxidation were monitored in mice overexpressed with constitutively active FoxO6 allele and FoxO6-null mice. For the in vitro study, liver cells overexpressing constitutively active FoxO6 and FoxO6-siRNA were treated with high glucose, and lipid metabolism alterations were measured. ER stress–induced FoxO6 activation suppressed hepatic β-oxidation in vivo. The expression and transcriptional activity of peroxisome proliferator-activated receptor α (PPARα) were significantly decreased in the constitutively active FoxO6 allele. Otherwise, inhibiting β-oxidation genes were reduced in the FoxO6-siRNA and FoxO6-KO mice. Our data showed that the FoxO6-induced hepatic lipid accumulation was negatively regulated by insulin signaling. High glucose treatment as a hyperglycemia condition caused the expression of ER stress–inducible genes, which was deteriorated by FoxO6 activation in liver cells. However, high glucose-mediated ER stress suppressed β-oxidation gene expression through interactions between PPARα and FoxO6 corresponding to findings in the in vivo study—lipid catabolism is also regulated by FoxO6. Furthermore, insulin resistance suppressed b-oxidation through the interaction between FoxO6 and PPARα promotes hepatic steatosis, which, due to hyperglycemia-induced ER stress, impairs insulin signaling.

Key messages

Our original aims were to delineate the interrelation between the regulation of PPARα and the transcription factor FoxO6 pathway in relation to lipid metabolism at molecular levels.

- Evidence on high glucose promoted FoxO6 activation induced lipid accumulation in liver cells.
- The effect of PPARα activation of the insulin signaling.
- FoxO6 plays a pivotal role in hepatic lipid accumulation through inactivation of PPARα in FoxO6-overexpression mice.

Keywords FoxO6 · Lipogenesis · PPARα · ER stress · Insulin signaling

✉ Dae Hyun Kim
dhkim74@pusan.ac.kr; bioimmune@hanmail.net

1 Department of Food Science & Technology, College of Natural Resources and Life Science, Pusan National University, Miryang-Si, Gyeongsangnam-Do 50463, Republic of Korea

Introduction

The global prevalence of obesity and associated metabolic diseases has significantly increased recently [1, 2]. Insulin resistance is a pathological condition in which cells fail to respond to normal insulin signals to store glucose in the tissues. Owing to the reduced glucose uptake from tissues in response to insulin and the consequent increase in insulin secretion by pancreatic beta cells, hyperglycemia and hyper-insulinemia occur in the body's attempt to control glucose

homeostasis. Moreover, diabetics overproduce glucose and triglycerides, contributing to the twin abnormalities of this disease—hyperglycemia and hypertriglyceridemia [3]. However, how these actions of insulin are mediated and why they are inextricably linked to the pathogenesis of insulin resistance, the forerunner of type-2 diabetes, remain unclear. Endoplasmic reticulum (ER) stress also influences insulin resistance [4–7]. Nevertheless, the molecular mechanism by which ER stress–mediated Forkhead box O6 (FoxO6) can lead to hepatic steatosis needs further investigation.

FoxO transcription factors induce target genes involved in the regulation of cellular metabolic pathways. The FoxO subfamily of proteins, including FoxO1, FoxO3, FoxO4, and FoxO6, is characterized by a highly conserved, winged-helix DNA-binding motif. Furthermore, FoxO proteins act as Akt substrates that mediate insulin's inhibitory effect on key genes involved in cell survival, proliferation, differentiation, oxidative stress, and metabolism in mammals [8]. For instance, the phosphorylation of FoxO by Akt, in response to insulin or other growth factors, allows FoxO to be translocated from the nucleus to the cytoplasm [8–10]. Suppressed growth factor signaling activates FoxO due to the Akt-induced FoxO inhibition; certain elevated fatty acids, such as palmitate, activate FoxO via a distinct mechanism involving the c-Jun N-terminal kinase (JNK) pathway [11]. ER stress has been associated with the JNK pathway through IRE1-mediated activation of JNK signaling [12, 13]. JNK phosphorylates the insulin receptor substrate (IRS) proteins and limits the activation of phosphatidylinositol 3-kinase (PI3K)/Akt signaling in response to insulin.

Conversely, the function of FoxO6 in hepatic lipid metabolism and its possible contribution to hypertriglyceridemia in type 2 diabetes remain unclear. Although increased ER stress results in insulin resistance, the molecular mechanism by which ER stress causes aberrant insulin responses has not been completely elucidated. This study reports a similar mechanism for ER stress that acts via the protein kinases inositol-requiring enzyme 1 (IRE1) and PKR-like ER kinase (PERK), which override the insulin-mediated inhibition of FoxO6 activity. ER stress has been suggested to be a crucial common factor in hepatic lipogenesis, liver-specific inflammation, and insulin resistance [14, 15]. ER stress also induces serine phosphorylation of IRS1 via the JNK pathway, inhibits insulin response in cultured liver cells [13, 16], enhances lipogenesis, affects hepatic steatosis, and influences insulin resistance [17]. Nonetheless, these inferences were drawn from studies conducted in genetically obese or prolonged chronic high-fat feeding models [13, 18], which have not provided reasonable insights into the effect of ER stress on de novo lipogenesis or lipid influx. The unfolded protein response (UPR) is induced by the accumulation of unfolded protein aggregates or excessive protein trafficking [19, 20]. Arsenic can activate the UPR, initiated by IRE1,

PERK, and ATF6 [21]. ATF4, ATF6, and XBP1 regulate the transcription of several genes, such as CHOP10—one of the genes highly expressed during ER stress [20]. However, C/EBPβ initially induces the expression of peroxisome proliferator-activated receptor γ (PPARγ) and C/EBPα, which then form a positive feedback loop by activating each other's expression and contribute to the induction and maintenance of expression of adipocyte-specific genes [22, 23]. Emerging evidence has demonstrated that PPARs regulate various cellular processes, including senescence, metabolism, and inflammation. Therefore, there is a cause to investigate the potential relationship between ER stress–mediated FoxO6 and other PPARα-related molecules in liver cells.

PPARs belong to the nuclear hormone receptor superfamily comprising ligand-modulated transcription factors. PPARs heterodimerize with retinoid X receptors (RXRs) and bind to PPAR response elements (PPRE) in the promoter region of specific target genes, regulating their transcription. Currently, three PPAR subtypes—PPARα, PPARβ, and PPARγ—have been identified. Among them, PPARγ promotes adipogenesis, controls lipid accumulation in adipocytes, and regulates the expression of adipocyte-secreted proteins and adipocytokines (leptin and adiponectin) to reduce lipotoxicity [24] and hepatic lipid metabolism [25, 26]. Kim et al. [27] reported that, in diabetic db/db mice, hepatic FoxO6 significantly induced hepatic PPARγ expression in insulin-resistant liver and hepatic lipogenesis and increased hepatic fat content. Accumulating evidence indicates that PPARα activation also participates in the regulation of cell apoptosis besides lipid metabolism and inflammation in cardiovascular diseases. PPARα agonist fenofibrate could prevent high glucose-induced apoptosis of VECs [28]. The apoptosis of vascular smooth muscle cells (VSMCs) induces the plaque vulnerability involved in cardiovascular diseases [29]. PPARα activation by agonists or overexpression of PPARα could regulate the apoptosis of VSMCs [30, 31]. Nevertheless, a molecular interaction between FoxO6 and PPARα in lipid accumulation by ER stress has not been reported. Alterations in lipid metabolism have been implicated in various metabolic diseases [32]. PPARα is the key transcriptional factor that regulates intracellular lipids through direct transcriptional control of genes involved in peroxisomal and mitochondrial fatty acid oxidation pathways, fatty acid uptakes, and TG catabolism [33, 34]. Accumulating evidence supports a link between PPARα and metabolic diseases, including diabetes, obesity, dyslipidemia, and fatty liver [34].

PPARα expression is enriched in tissues with high fatty acid oxidation (FAO) rates, such as the liver, heart, skeletal muscle, brown adipose tissue, and kidneys, and is expressed in many tissues and cells, including the intestine, vascular endothelium, and smooth muscle and immune cells (e.g., monocytes, macrophages, and lymphocytes) [33]. PPARα is

a nutritional sensor that allows adaptation of the rates of fatty acid (FA) catabolism, lipogenesis, and ketone body synthesis in response to feeding and starvation [35]. PPARα is a transcriptional regulator of genes involved in peroxisomal and mitochondrial β-oxidation, FA transport, and hepatic glucose production, the latter being rodent-specific [36]. PPARα ligands are FA derivatives formed during lipolysis, lipogenesis, or FA catabolism. Substrates of the first rate-limiting peroxisomal β-oxidation enzyme, acyl-CoA oxidase 1 (ACOX1), are likely PPARα agonists. Consistently, disruption of ACOX1 in mice results in increased peroxisome proliferation, hepatocarcinoma, and elevated PPARα target gene expression [37, 38]. The oxidized phospholipid fraction of oxidized low-density lipoprotein (LDL) enhances PPARα transcriptional activity and induces its target gene, FATP-1, in human primary endothelial cells [39]. Liver-specific knockout of fatty acid synthase (FAS), an enzyme catalyzing the synthesis of FA, resulted in hypoglycemia and liver steatosis when mice were fed a fat-depleted diet, which was reversed by dietary fat or a synthetic PPARα agonist, identifying products of FAS-dependent de novo lipogenesis as PPARα activators [40]. In rodents and primates, FA transport across the mitochondrial membrane is triggered by PPRE-dependent regulation of CPT-I and CPT-II, in which proteins are localized in the outer and inner mitochondrial membrane, respectively.

This study investigated the role of FoxO6 in downregulating PPARα expression through ER stress in the liver and liver cells to form a better understanding of the molecular mechanisms involved in hepatic lipogenesis.

Materials and methods

Materials

Except where noted otherwise, all chemical reagents were obtained from Sigma (St. Louis, MO, USA). Western blotting detection reagents were obtained from Amersham (Bucks, UK), and RNAzol™ B was obtained from Tel-Test Inc. (Friendswood, TX, USA). Antibodies against α-tubulin (sc-5286), β-actin (sc-47778), TFIIB (sc-271736), p-Akt (sc-101629), total-Akt (sc-1618), p-PERK (sc-32577), PERK (sc-13073), IRE (sc-390960), ATF6 (sc-22799), pS-IRS (sc-33956), pT-IRS (sc-17196), and IRS (sc-559) were obtained from Santa Cruz Biotechnology (Santa Cruz, CA, USA). Antibodies against p-IRE (ab48187), PPARα (ab24509), CPT1α (ab128568), and ACOX1 (ab184032) were purchased from Abcam (Cambridge, UK). Antibodies against FoxO6 and p-FoxO6 (Ser184) were obtained from Dr. Dong (University of Pittsburgh, Pittsburgh, PA, USA). Horseradish peroxidase–conjugated anti-rabbit IgG and horseradish peroxidase–conjugated anti-mouse IgG antibodies were

obtained from Amersham (Bucks, UK). Horseradish peroxidase–conjugated anti-sheep/goat IgG from donkey was purchased from Serotec (Oxford, UK). Polyvinylidene difluoride (PVDF) membranes were obtained from Millipore Corporation (Bedford, MA, USA). PPARα-siRNA (20 nM) was obtained from Integrated DNA Technologies (IDT; Coralville, Iowa).

Animal experimental procedures

The FoxO6-overexpression (FoxO6-Tg) and FoxO6-knockout (FoxO6-KO) male mice aged 8 weeks were fed standard rodent chow or a high-fat diet (fat content, 60 kcal%; Research Diets, Inc., New Brunswick, NJ), depending on the group they were in, and were provided water ad libitum. The mice were kept in sterile cages, with a 12-h light/dark cycle. The livers from the FoxO6-Tg and FoxO6-KO mice were obtained from the University of Pittsburgh Medical Center (Dr. Dong, University of Pittsburgh, PA, USA).

Cell culture

Human hepatoma cells line (HepG2 cells) were purchased from the American Type Culture Collection (ATCC, VA, USA). Cells were cultured in Dulbecco's modified Eagle's medium (DMEM, Lonza, Walkersville, MD) and were transduced with an Adv-FoxO6-CA vector expressing the constitutively active FoxO6 allele, as previously described [41]. The Adv-Empty vector was used as a control. Previous research has described the Adv-FoxO6-siRNA vector expressing the FoxO6-specific siRNA and Adv-Sc-siRNA vector encoding scrambled siRNA [41]. The Adv-Akt-CA vector encodes a constitutively active form of Akt [42], and all adenoviral vectors were produced in HEK293 cells [43].

Transfection and luciferase assay

The HepG2 cells were purchased from the American Type Culture Collection (ATCC, VA, USA). Cells were cultured in Dulbecco's modified Eagle's medium (DMEM, Lonza, Walkersville, MD). For a peroxisome proliferator response element (PPRE; 5′-GATCCCCGAACGTGACCT TTGTCCTGGTCC-3′)-driven luciferase assay, 1×10^4 HepG2 cells were seeded per well into a 48-well cell culture plate. The PPRE-X3-TK-LUC plasmid (0.5 μg) (a kind gift from Dr. Christoper K. Glass, University of California, San Diego, CA, USA) and 0.05 μg of full-length human PPARα expression vectors (kind gifts from Dr. Han Geuk Seo, Konkuk University, Seoul, South Korea) were transfected into the cells using 0.5 μg DNA/0.5 μl Lipofectamine

2000 (Invitrogen, Carlsbad, CA, USA) complexes in 500 μl normal media containing 10% serum, incubated for 24 h, and treated with the scrambled or FoxO6-CA (100 MOI). After incubation, the transfection medium was replaced with a fresh medium. Subsequently, 25 mM of glucose was added, and after 24 h incubation, the cells were washed with phosphate-buffered saline (PBS). Luciferase activity was analyzed using the Steady-Glo Luciferase Assay System (Promega, Madison, WI, USA) and was measured using a luminometer (GENious, TECAN, Salzburg, Austria).

Western blot analysis

The homogenized samples were boiled for 5 min with a gel-loading buffer (0.125 M Tris–HCl, pH 6.8, 4% sodium dodecyl sulfate (SDS), 10% 2-mercaptoethanol, and 0.2% bromophenol blue) at a 1:1 ratio. Equal amounts of total protein from each sample were separated by SDS–polyacrylamide gel electrophoresis (SDS-PAGE) using 10% acrylamide gels and transferred to PVDF membranes at 80 V for 1.5 h in a semi-dry transfer system. The membranes were immediately placed in a blocking buffer (5% non-fat milk in 10 mM Tris at pH 7.5, 100 mM NaCl, and 0.1% Tween 20). The blot was blocked at room temperature for 30 min. The membrane was incubated with a specific primary antibody at 4 °C overnight, followed by a horseradish peroxidase–conjugated anti-rabbit antibody at room temperature for 1.5 h. Labeled antibodies were detected using WESTSAVE™ (Abfrontier, South Korea). Pre-stained protein markers were used for molecular weight determinations.

Hepatic lipid content

Liver tissues or cells (20 mg) were homogenized in 400 μl of HPLC-grade acetone. After an overnight incubation with agitation at room temperature, 50 μl aliquots of acetone-extracted lipid suspensions were used to determine triglyceride concentrations via the infinity triglyceride reagent (Thermo Electron). As described earlier, hepatic lipid content was defined as milligrams of triglyceride per gram of total liver proteins(Kamagate et al., 2008; Qu et al., 2006).

RNA isolation and real-time quantitative reverse transcriptase PCR (qRT-PCR)

RNA was isolated from liver tissue or cells using the RNeasy Mini Kit (QIAGEN, Valencia, CA). qRT-PCR analysis was performed to quantify mRNA concentrations using the SYBR Green and the CFX Connect System (Bio-Rad Laboratories Inc., Hercules, CA, USA). Supplementary Table 1 shows the primers used. All primers were purchased from IDT (Coralville, IA). The $2^{-\Delta\Delta Ct}$ method was used to calculate the fold changes. The *Gapdh* gene served as a reference gene.

Immunoprecipitation (IP) of tissue extracts

Liver tissue extracts were immunoprecipitated in a buffer containing 40 mM Tris–HCl (pH 7.6), 120 mM NaCl, 20 mM glycerophosphate, 20 mM NaF, 2 mM sodium orthovanadate, 5 mM ethylenediaminetetraacetic acid (EDTA), 1 mM phenylmethylsulfonyl fluoride (PMSF), 0.1% NP40 containing leupeptin (2 μg/ml), aprotinin (1 μg/ml), and pepstatin A (1 μg/ml). Aliquots of cell extracts were centrifuged at $12,000 \times g$ at 4 °C for 15 min and incubated overnight at 4 °C with the required antibody and at 4 °C in a 50% protein A agarose slurry. After washing the immunoprecipitates three times with IP buffer, immunoprecipitated proteins were analyzed using SDS-PAGE, and Western blotting analysis was performed as described above.

Histological analysis

The Oil Red O staining was performed with optimal cutting temperature of frozen tissues to visualize lipid accumulation.

Immunostaining

HepG2 cells were seeded at 1×10^4 cells per well in a 6-well plate, incubated for 24 h, fixed in 4% paraformaldehyde solution (15 min at room temperature), washed with PBS buffer, blocked with 3% normal goat serum (Gibco, Grand Island, USA), and immunostained using a rabbit anti-PPARα antibody (1:500 dilution) at 4 °C overnight. Subsequently, the cells were washed with TBS and incubated for 3 h in the presence of anti-rabbit IgG labeled with Alexa Fluor 488 (1:200; Invitrogen, CA, USA). The cell nuclei were visualized by immunostaining with Hoechst 33,342 (1:1000; Invitrogen), and PPARα localization was determined by confocal laser scanning microscopy (TCS SP2, Leica, Wetzler, Germany).

Statistical analyses

The *t* test was used to analyze differences between the two groups, and treatments were compared by one-way analysis of variance (ANOVA) followed by Dunnett's post-hoc test. *p*-values < 0.05 were considered statistically significant. The analysis was performed using GraphPad Prism 5 (GraphPad software).

Results

ER stress–mediated lipid accumulation through the interaction between FoxO6 and PPARα

The transcriptional activities of FoxO family proteins have been previously demonstrated to increase when insulin levels are reduced [9]. We examined the expression of ER stress genes in glucose concentration-treatment liver cells. To examine the hypothesis that insulin signaling transactivates ER stress genes, we conducted studies to assess the glucose-induced expression of ER stress genes in HepG2 cells. The results showed that glucose construction enhanced p-IRE, p-PERK, ATF6, and p-JNK levels (Supp. Figure 1).

We further explored the relationships between FoxO6 and PPARα. To this end, serum-starved liver cells were treated with 25 mM glucose. We found that FoxO6 levels increased in glucose-treated groups, and nuclear protein levels of PPARα and target genes, such as ACOX1 and CPT1α, were reduced in the liver cells of high glucose (Fig. 1A). Additionally, our immunoprecipitation experiments showed that the interaction between FoxO6 and PPARα was suppressed in the high glucose groups (Fig. 1B). Moreover, high glucose inhibited the transcriptional activation of PPARα, as determined by PPARα luciferase assay in human liver cells (Fig. 1C). These results were confirmed by liver cell Oil Red O staining—lipid accumulates in high glucose-treated cells (Fig. 1D). We explored the effect of high glucose on lipid accumulation in liver cells and found a remarkable high glucose increase in TG concentration (Fig. 1E). Nevertheless, the target genes of β-oxidation PPARα (e.g., CPT1α) and acyl-CoA oxidase (ACOX) decreased in high glucose (Fig. 1F). We examined insulin signaling in the liver. As shown in Fig. 1G, phosphorylated IRS and phosphorylated Akt were found to decrease with high glucose (Fig. 1G).

FoxO6 is a transcription factor negatively regulated by Akt during insulin signaling. FoxO6 dephosphorylation enhances its stability and activity, stimulating gluconeogenesis and hyperlipidemia. PPARα expression was increased by various concentrations of a constitutively active form of Akt (CA-Akt) (Supp. Figure 2).

ER stress–mediated FoxO6 activation decreases β-oxidation by suppressing PPARα in liver cells

To determine whether FoxO6 influences the functional relationships between lipogenesis genes and aberrant ER stress, treatment of cells with ER stress activators (tunicamycin) induced ER stress genes (Supp. Figure 3A). However, our immunoprecipitation experiments showed

that an interaction between FoxO6 and PPARα was suppressed in the tunicamycin groups. Phosphorylation of FoxO6 (inactivation form) decreased in tunicamycin-treated groups (Supp. Figure 3B). Further, tunicamycin was accompanied by decreased expression of CPT and ACOX1 (Supp. Figure 3C), two key enzymes involved in fatty acid oxidation through PPARα. We examined PAR2 expression in HepG2 cells exposed to the FoxO6 virus. Cells were treated with or without different concentrations of FoxO6-carrying viruses (20–500 MOI). Treatment with 20–500 MOI of FoxO6 suppressed PPARα expression (Supp. Figure 4).

We employed a viral system for the exogenous overexpression of FoxO6 in liver cells. Liver cells were intravenously transfected with a constitutively active form of FoxO6 (FoxO6-CA) or empty vector, and ER stress was assessed. We examined the expression of ER stress genes in FoxO6 virus-transduced liver cells. As shown in Fig. 2A, treatment with 100 MOI FoxO6 suppressed PPARα levels. However, the β-oxidation gene, ACOX1, was affected in FoxO6-transduced hepatocytes (Fig. 2A). We used the liver cell line to investigate the functional role of FoxO6 in hepatic steatosis. Specifically, we hypothesized that FoxO6-induced lipid accumulation in the liver occurs, at least in part, via PPARγ activation. As a transcription factor, PPARγ influences hepatic steatosis by inducing lipogenesis-related gene expression [44, 45]. We explored the effect of FoxO6 overexpression on lipid accumulation in liver cells and found a remarkable FoxO6-dependent increase in TG concentration (Fig. 2B). These results were confirmed by liver cell Oil Red O staining—fat accumulates in FoxO6-overexpressing cells (Fig. 2C). The target genes of β-oxidation PPARα (e.g., CPT1α) and ACOX were decreased in FoxO6-CA (Fig. 2D). Additionally, our immunoprecipitation experiments showed that the interaction between FoxO6 and PPARα was suppressed in FoxO6-CA (Fig. 2E). Furthermore, FoxO6 caused the transcriptional activation of PPARα, as determined by PPARα luciferase assay in HepG2 cells (Fig. 2F). Based on these findings, we suggest that FoxO6 induces lipid accumulation through the downregulation of β-oxidation genes.

PPARα deficiency blunt liver lipid accumulation in liver cells

To confirm the role of PPARα in FoxO6-CA-induced lipid accumulation, we subjected liver cells to PPARα-siRNA and FoxO6-CA and compared changes in lipid metabolism. As expected, FoxO6-CA showed decreased PPARα gene expression (Fig. 3A). Compared with FoxO6-CA, PPARα-siRNA led to reduced expression of β-oxidation-associated proteins (Fig. 3A). In liver cells, FoxO6 activity suppressed
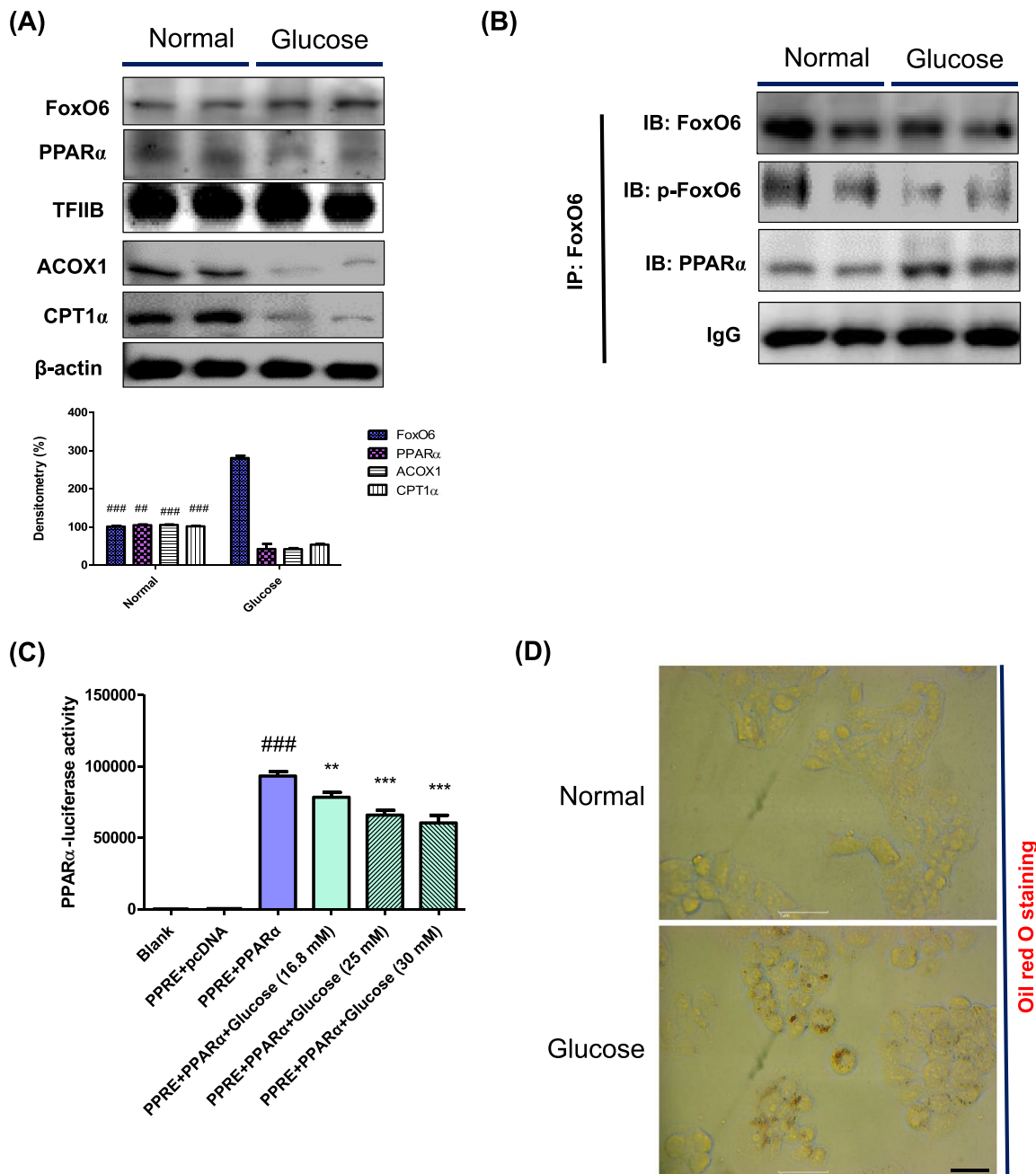
Fig. 1 High glucose-induced ER stress–mediated lipid accumulation. **A** Western blot analysis was used to detect FoxO6, PPARα, ACOX1, and CPT1α in nuclear extracts and cytosolic from liver cells. TFIIB was the loading control of the nuclear fraction. β-actin acts as the loading control for the cytosolic fractions. One-factor ANOVA was used to determine the significant differences. $^{##}p<0.01$, $^{###}p<0.001$ vs. glucose-treated HepG2 cells. **B** Western blot analysis showed that immunoprecipitated FoxO6 and PPARα were physically associated with PPARα and FoxO6, respectively. **C** Effect of glucose on the activity of the PPARα promoter. HepG2 cells in 48-well microplates were transduced with glucose (25 mM), followed by transfection with 0.05 μg of pcDNA and PPARα DNA in the culture medium. After a 24-h incubation, the cells were harvested. The relative luciferase activity was calculated based on the PPARα luciferase/β-galactosidase activity ratio. The data are expressed as a mean±SEM. $^{$$$}p<0.001$ vs. pcDNA treated cells; $^{###}p<0.001$ vs. PPRE-treated cells; and $^{**}p<0.01$, $^{***}p<0.001$ vs. PPRE with PPARα DNA-treated cells. **D** Liver cells were stained with Oil Red O to visualize lipid accumulation by high glucose. Scale bar, 100 μm. **E** Cellular triglyceride concentration after treatment with glucose (25 mM) for 24 h was measured by a colorimetric assay. The data are expressed as a mean±SEM. $^{###}p<0.001$ vs. glucose-treated cells. **F** Real-time PCR analyses were performed to measure the mRNA levels of β-oxidation genes (PPARα, CPT1α, and ACOX1). The data are expressed as a mean±SEM. $^{*}p<0.05$ vs. glucose-treated cells. **G** Western blot was used to detect pSer-IRS1, pTyr-IRS1, IRS1, p-Akt, and Akt in cytoplasmic extracts (20 μg protein) after treatment of liver cells with glucose (25 mM) for 6 h. β-actin was the loading control of the cytosolic fractions. One-factor ANOVA was used to determine the significant differences. $^{#}p<0.05$ and $^{###}p<0.001$ vs. glucose-treated HepG2 cells

(E)

Cellular TG

(F)
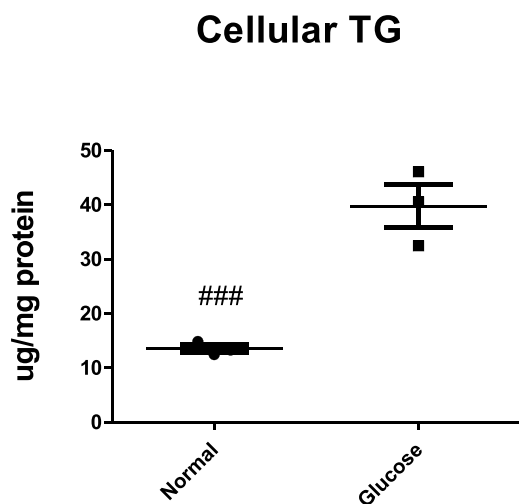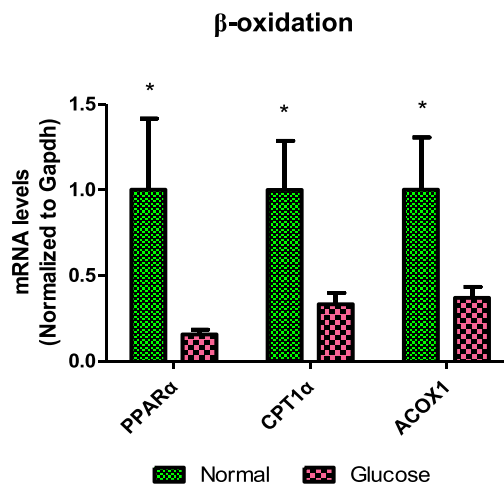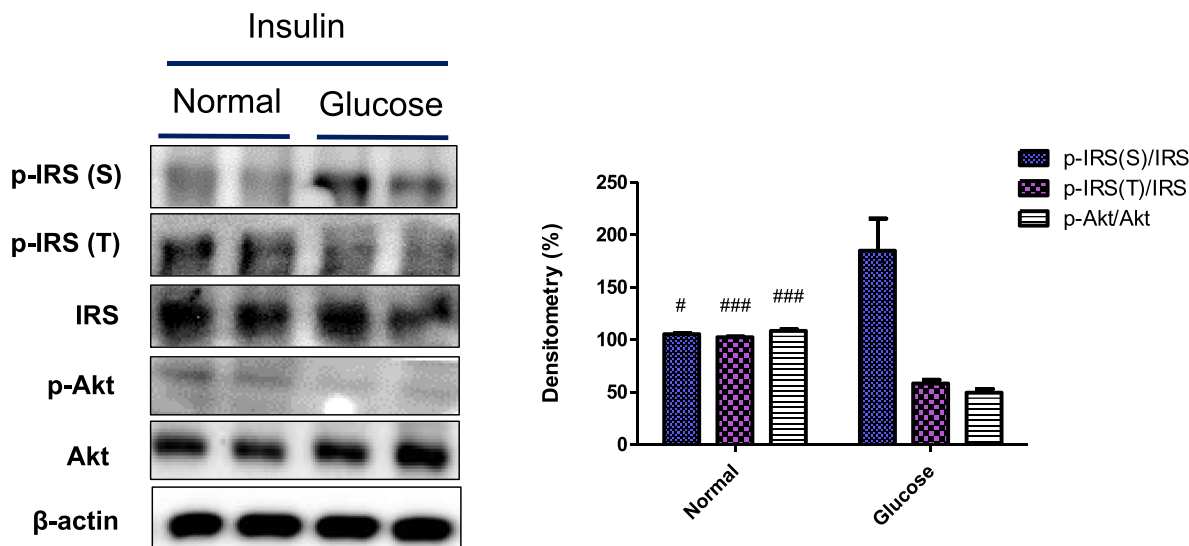
β-oxidation

(G)

Fig. 1 (continued)

PPARα transcriptional activity, as assessed by immunofluo-rescence staining (Fig. 3B). However, FoxO6-CA combined with PPARα-siRNA led to significantly lower β-oxidation genes (e.g., PPARα, CPT1α, and ACOX) compare with FoxO6-CA alone (Fig. 3C). FoxO6-CA combined with PPARα-siRNA led to significantly higher cellular TG compared with FoxO6-CA alone (Fig. 3D). These data indicate that PPARα deficiency significantly decreases β-oxidation with high lipid accumulation in liver cells.

Decrease of hepatic TGs through PPARα activation in FoxO6-siRNA transfected cells

To further establish the importance of FoxO6 in ER stress, we employed siRNA-mediated gene silencing to knock down FoxO6 expression in liver cells. We also meas-ured FoxO6 and PPARα levels using Western blotting. Significant differences in the expression levels of FoxO6 and PPARα were observed in the FoxO6-deficient cells

(A)
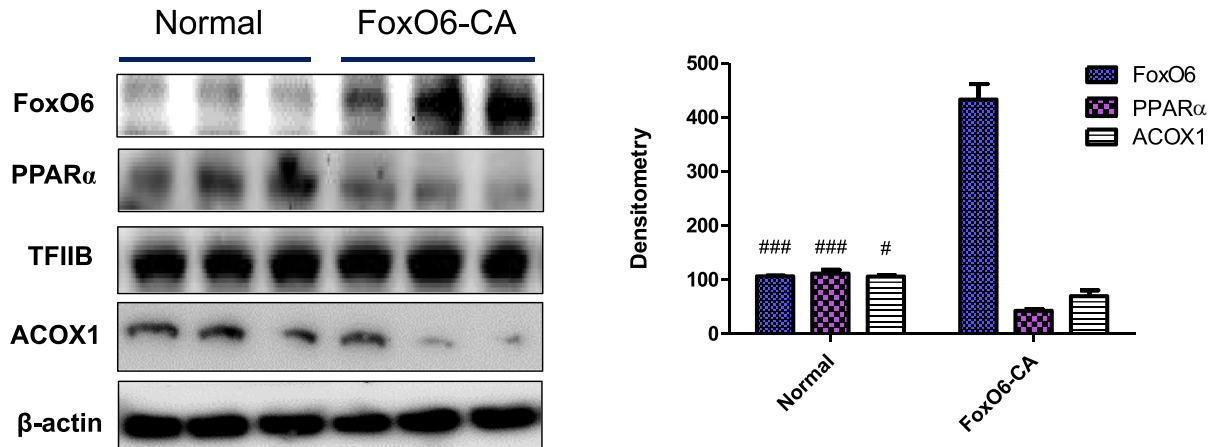
(B)
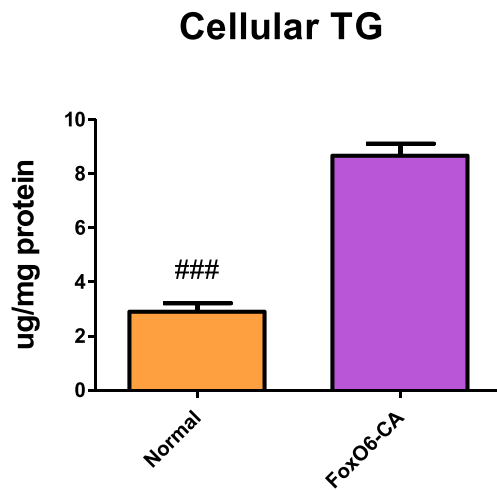
(C)
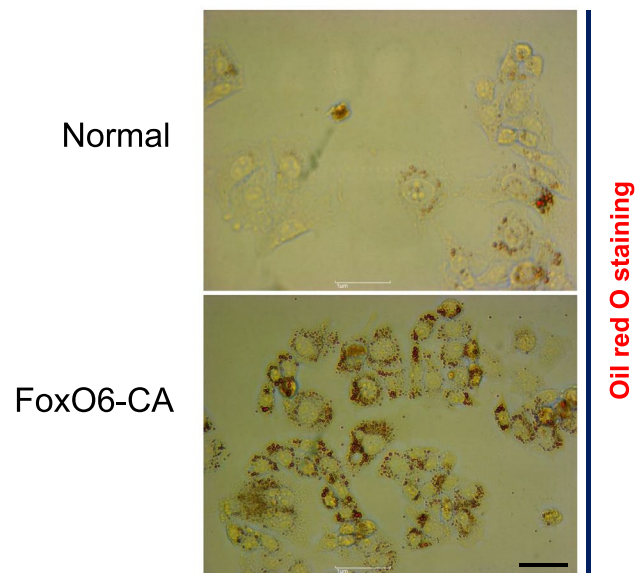
Fig. 2 FoxO6 regulates lipid accumulation in FoxO6-virus-treated cells. **A** Inactivation of PPARα by FoxO6. Liver cells were grown to 80% confluence in 100-mm dishes in DMEM and then stimulated with 100 MOI FoxO6 and analyzed by Western blotting using the appropriate antibody. TFIIB was the loading control of the nuclear fraction. β-actin acts as the loading control for the cytosolic fractions. One-factor ANOVA was used to determine the significant differences. $^{\#}p < 0.05$ and $^{\#\#\#}p < 0.001$ vs. FoxO6-CA-treated HepG2 cells. **B** Cellular triglyceride levels by FoxO6-CA in cells. Results of one-way ANOVA: $^{\#\#\#}p < 0.001$ vs. FoxO6-CA vector. **C** Liver cells were stained with Oil Red O to visualize lipid accumulation. Scale bar, 100 μm. **D** β-oxidation genes were subjected to real-time qRT-PCR analysis. Results of the one-way ANOVA: $^{*}p < 0.05$ vs. FoxO6-CA vector. **E** Western blotting showed that immunoprecipitated FoxO6 and PPARα were physically associated with PPARα and FoxO6, respectively. **F** HepG2 cells in 48-well microplates were transduced with AdV-FoxO6 or control AdV-null vectors at a fixed dose (MOI, 100 pfu/cell), followed by transfection with 0.05 μg of pcDNA and PPARα DNA in the culture medium. After a 24-h incubation, the cells were harvested. The relative luciferase activity was calculated based on the PPARα-luciferase/β-galactosidase activity ratio. The data are expressed as a mean ± SEM. $^{\#\#\#}p < 0.001$ vs. PPRE-treated cells; $^{**}p < 0.01$ and $^{***}p < 0.001$ vs. PPRE with PPARα DNA-treated cells
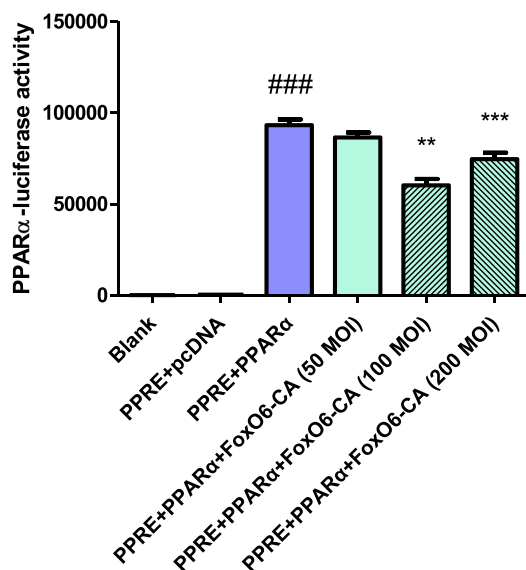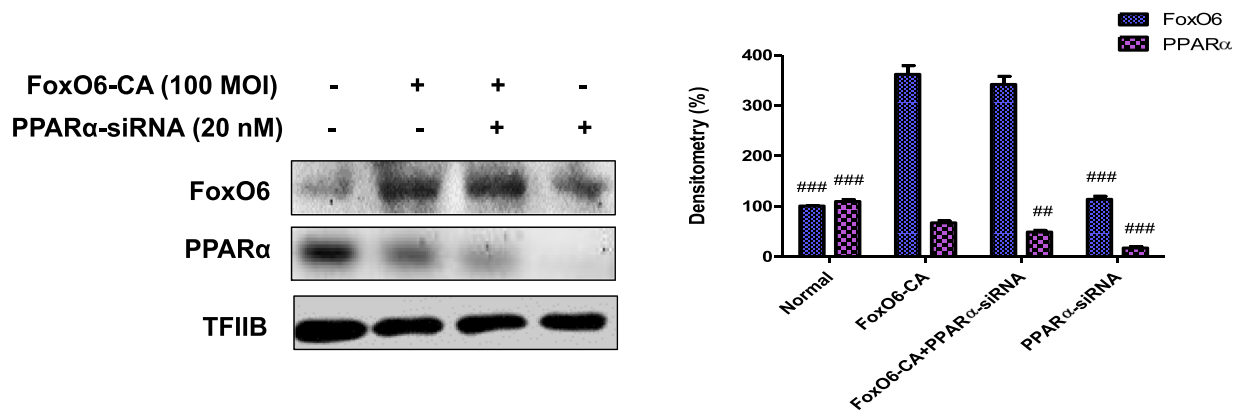
(D)
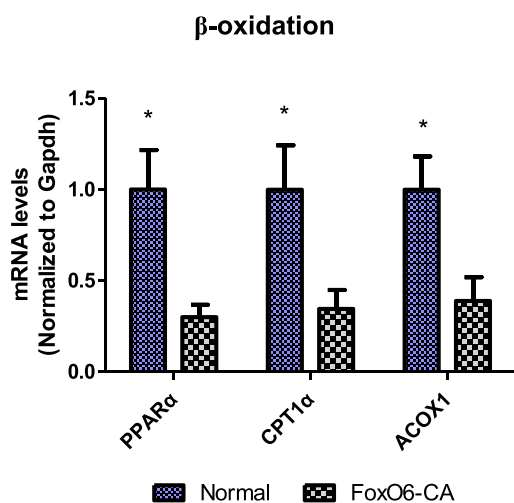
(E)
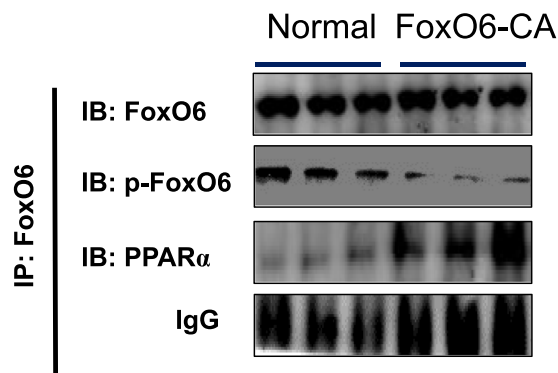
(F)

Fig. 2 (continued)

(Fig. 4A). We explored the effect of FoxO6-deficient on lipid accumulation in liver cells and found remarkable FoxO6-siRNA suppression in TG concentration (Fig. 4B). The target gene of β-oxidation PPARα was increased in FoxO6-siRNA (Fig. 4C). Considered together, these results suggested that the knockdown of FoxO6 partially prevented hyperglycemia-induced activation of lipogenesis genes.
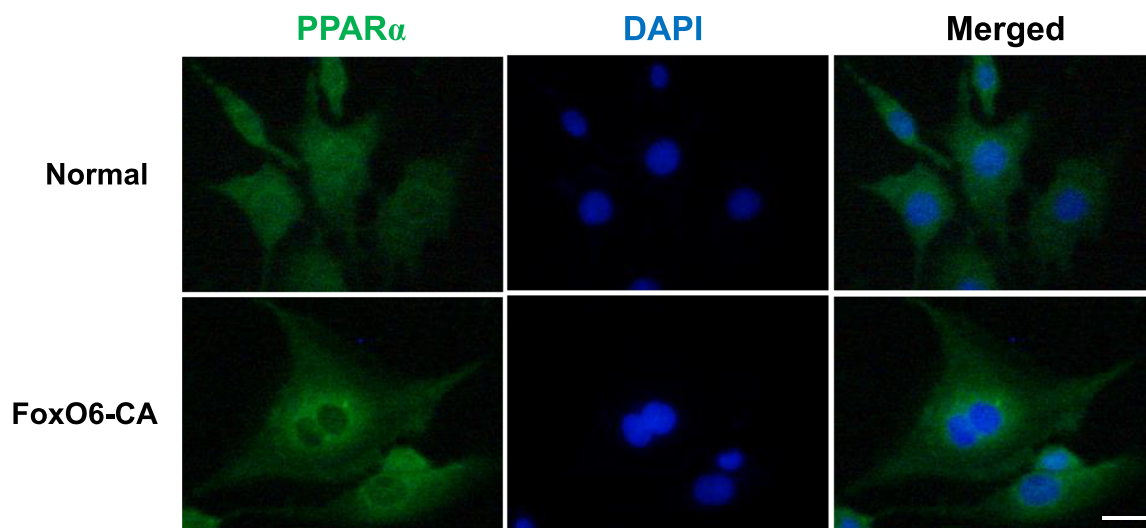
Effect of hepatic TGs in Akt inhibitor and metformin-treated cells

We examined PPARα expression in HepG2 cells exposed to Akt inhibitor and metformin. Akt was suppressed for 4 h after LY294002 treatment at 30 μM. Levels of PPARα expression decreased when cells were treated with

(A)

FoxO6-CA (100 MOI)   -   +   +   -
PPARα-siRNA (20 nM)   -   -   +   +

FoxO6

PPARα

TFIIB

(B)

PPARα   DAPI   Merged

Normal

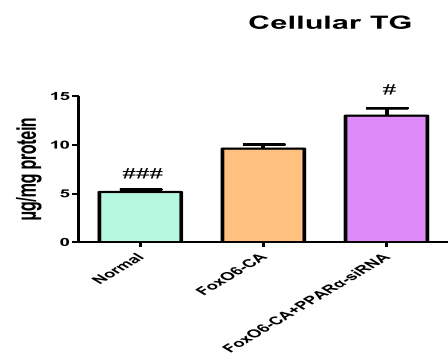FoxO6-CA

(C)

β-oxidation

(D)

Cellular TG
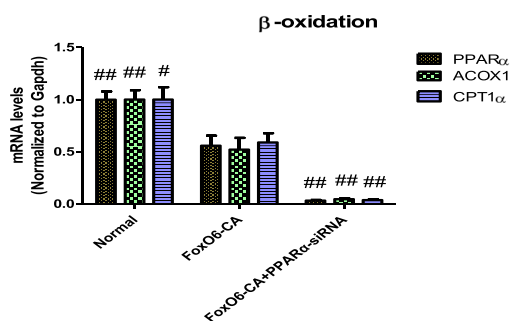
**Fig. 3** FoxO6 regulates lipid accumulation through PPARα in FoxO6-virus with PPARα-siRNA-treated cells. **A** AC2F cells were grown to 80% confluence in 100-mm dishes containing DMEM, pre-treated (1 day) with or without PPARα-siRNA (20 nM), then stimulated with the FoxO6 virus (100 MOI) for 1 day. Western blotting was used to detect FoxO6 and PPARα in whole extracts (20 μg protein) by using the β-actin as a control from liver cells. One-factor ANOVA was used to determine the significant differences. $^{##}p < 0.01$, $^{###}p < 0.001$ vs. FoxO6-CA-treated HepG2 cells. **B** Liver cells were treated with FoxO6 vector for 24 h. Cells were immunostained using rabbit anti-PPARα antibody followed by IgG conjugated with fluorescein isothiocyanate (green). Bar = 50 μm. Liver cells were grown to 80% confluence in 100-mm dishes containing DMEM, pre-treated (1 day), and then stimulated with the FoxO6 virus (100 MOI) for 1 day. **C** β-oxidation genes were subjected to real-time qRT-PCR analysis. Results of the one-way ANOVA: $^{#}p < 0.05$ and $^{##}p < 0.01$ vs. FoxO6-CA vector. **D** Triglyceride levels in cells. Results of the one-way ANOVA: $^{#}p < 0.05$ and $^{###}p < 0.001$ vs. FoxO6-CA vector

(A)
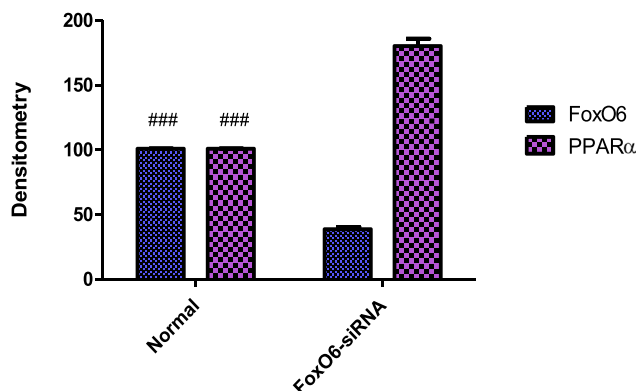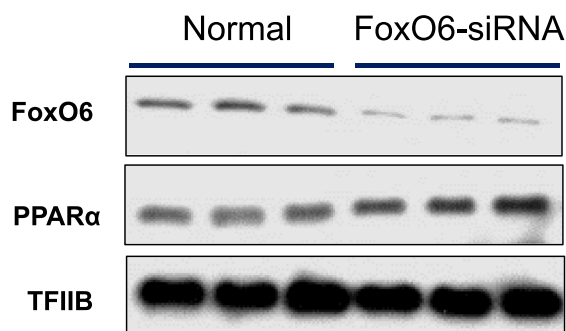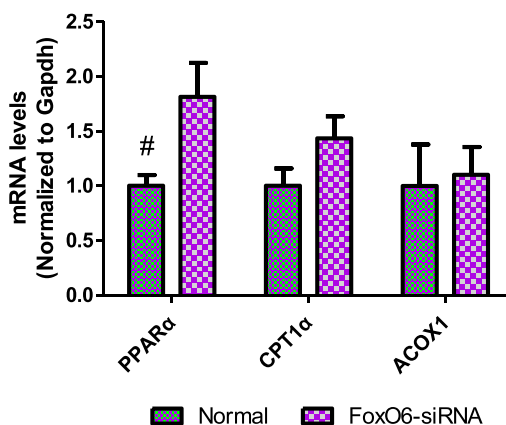

(B)
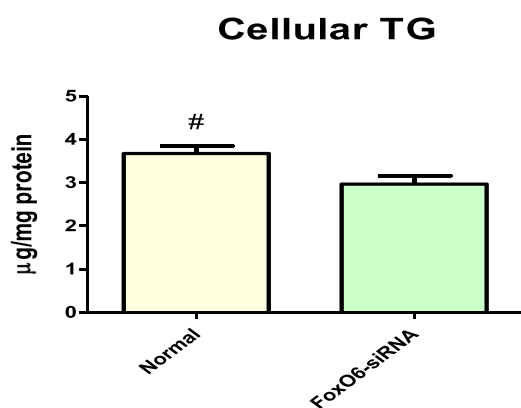
(C)

Fig. 4 Effect of FoxO6 deletion on the regulation of lipid metabolism. **A** Western blot analysis was used to detect FoxO6 and PPARα in FoxO6-siRNA-treated liver cells. β-actin was used as a loading control. One-factor ANOVA was used to determine the significant differences. $^{###}p < 0.001$ vs. FoxO6-siRNA-treated HepG2 cells. **B** Liver cells were treated with FoxO6-siRNA (100 MOI) for 24 h. Triglyceride levels were quantified in the liver cells. $^{#}p < 0.05$ vs.

FoxO6-siRNA-treated HepG2 cells. **C** The expression of PPARα, CPT1, and ACOX1 was analyzed by qRT-PCR after 24 h in FoxO6-siRNA-transfected (100 MOI) cells. The results were normalized based on the Gapdh level. One-factor ANOVA was used to determine the significant differences. $^{#}p < 0.05$ vs. FoxO6-siRNA-treated HepG2 cells

LY294002 (Fig. 5A). Moreover, our immunoprecipitation experiments showed that the interaction between FoxO6 and PPARα was increased in the high glucose with Akt inhibitor groups compare with the glucose-treated groups (Fig. 5B). We explored the effect of the Akt inhibitor on lipid accumulation in liver cells and found a remarkably high glucose level with Akt inhibitor increase in the TG

concentration (Fig. 5C). However, the Akt level was suppressed 24 h after metformin. Levels of PPARα expression dropped when cells were treated with metformin (Fig. 5D). We explored the effect of metformin on lipid accumulation in liver cells and found a remarkably high glucose level with metformin decrease in the TG concentration (Fig. 5E).
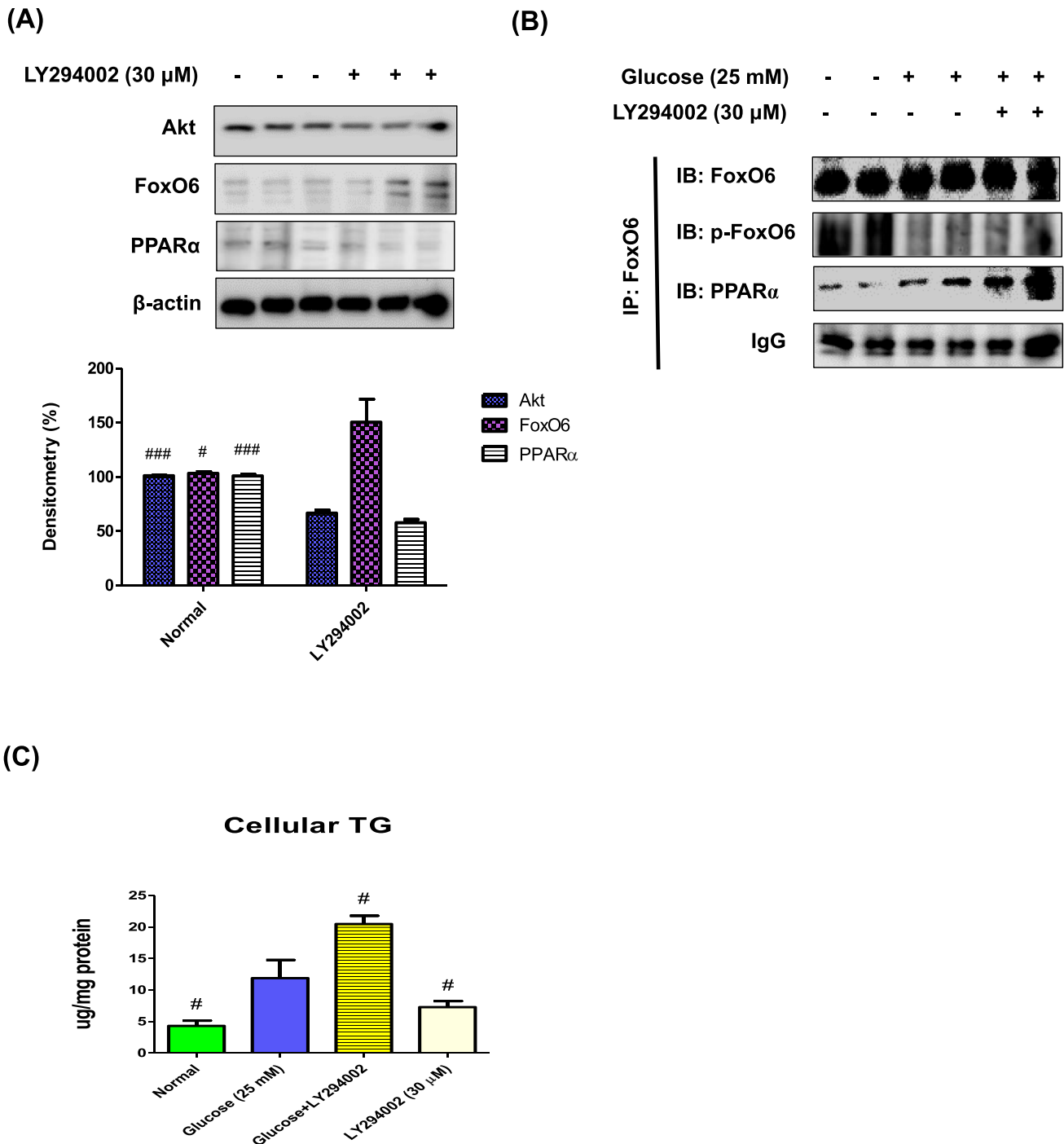
(A)

LY294002 (30 μM)   -   -   -   +   +   +

Akt

FoxO6

PPARα

β-actin

(B)

Glucose (25 mM)   -   -   +   +   +   +
LY294002 (30 μM)   -   -   -   -   +   +

IP: FoxO6

IB: FoxO6

IB: p-FoxO6

IB: PPARα

IgG

(C)

Cellular TG

Fig. 5 Lipid accumulation by Akt inhibitor and metformin in the liver. **A** Western blot analysis was used to detect Akt, FoxO6, and PPARα in whole extracts from Akt inhibitor-treated liver cells. β-actin was the loading control of the whole fraction. One-factor ANOVA was used to determine the significant differences. $^{#}p < 0.05$, $^{###}p < 0.001$ vs. LY294002-treated HepG2 cells. **B** The Western blot analysis showed that immunoprecipitated PPARα, FoxO6, and p-FoxO6 were physically associated with PPARα and FoxO6, respectively. **C** Cellular triglyceride levels by glucose with Akt inhibitor (LY294002) in cells. Results of the one-way ANOVA: $^{#}p < 0.05$ vs. glucose. **D** Western blot analysis was used to detect Akt, FoxO6, and PPARα in whole extracts from metformin-treated liver cells. β-actin was the loading control of the whole fraction. One-factor ANOVA was used to determine the significant differences. $^{###}p < 0.001$ vs. metformin-treated HepG2 cells. **E** Cellular triglyceride levels by glucose with metformin in cells. Results of the one-way ANOVA: $^{##}p < 0.01$, $^{###}p < 0.001$ vs. glucose
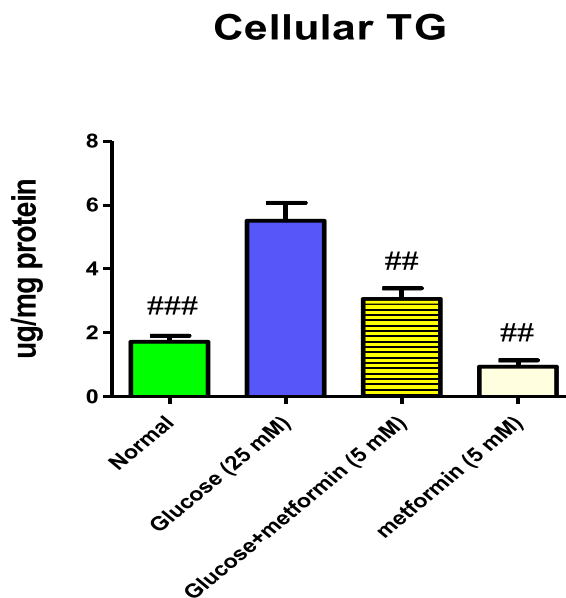
(D)
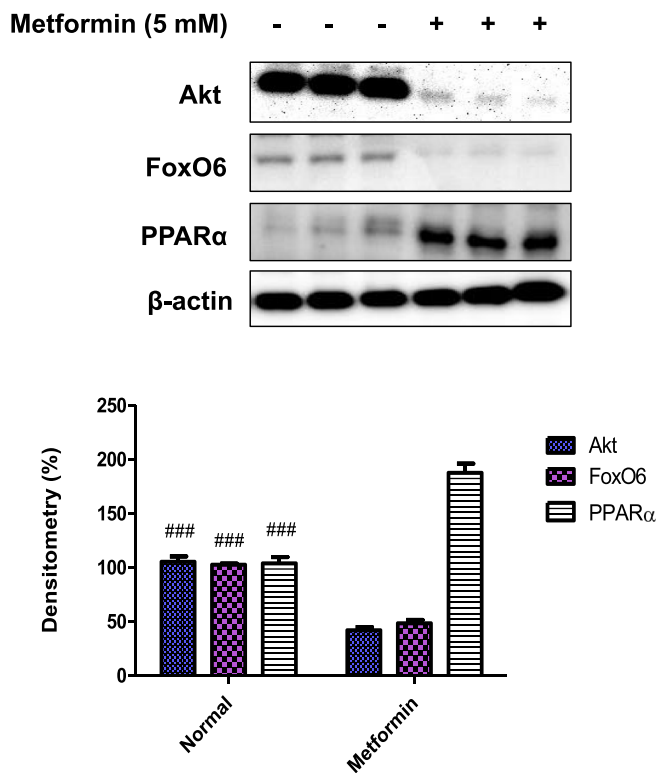
(E)

Fig. 5 (continued)

FoxO6 upregulates lipid accumulation through PPARα suppression in mice

To determine whether FoxO6 influences relating lipogenesis gene expression to aberrant ER stress and characterize the underlying mechanism, we determined the hepatic expression of genes involved in lipogenesis and fatty acid oxidation—two opposing pathways in hepatic lipid metabolism—in the FoxO6-Tg liver. FoxO6-Tg resulted in a significant reduction of β-oxidation, as reflected by the significantly decreased nuclear level of PPARα (Fig. 6A). FoxO6-Tg was accompanied by decreased expression of carnitine palmitoyltransferase (CPT) and acyl-coenzyme A oxidase 1 (ACOX1) (Fig. 6A), two key enzymes involved in fatty acid oxidation through PPARα. We measured the hepatic TG content and found that FoxO6-Tg mice were associated with increased fat content in the liver compared to their control littermates (Fig. 6B), which is consistent with the notion that FoxO6 promotes hepatic lipogenesis. Furthermore, our immunoprecipitation experiments showed that the interaction between FoxO6 and PPARα was suppressed in the FoxO6-Tg liver (Fig. 6C).

To characterize the role of FoxO6 in glucose metabolism, Calabuig-Navarro et al. [46] bred FoxO6$^{+/-}$ heterozygous mice to generate viable homozygous KO mice (FoxO6-KO). We analyzed the lipogenesis gene levels to determine the effect of lipid accumulation on FoxO6 depletion. Significant differences were observed in the expression levels of PPARα between FoxO6-KO and their wild-type (WT) littermates on a high-fat diet. FoxO6-KO increased the PPARα level in liver tissues (Supp. Figure 5A). We explored the effect of FoxO6-deficient on lipid accumulation in FoxO6-KO liver and found remarkable FoxO6-KO suppression in the TG concentration (Supp. Figure 5B).
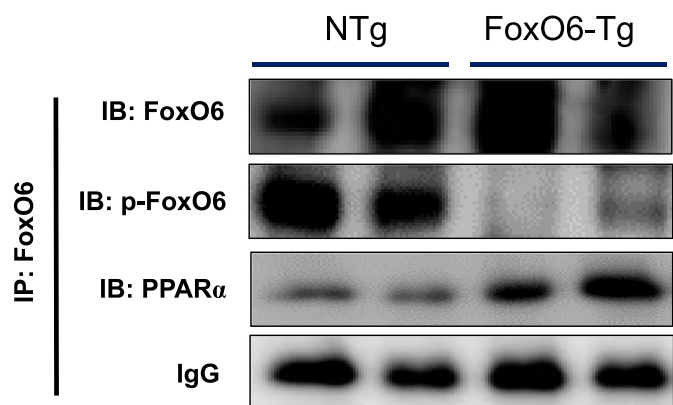
(A)
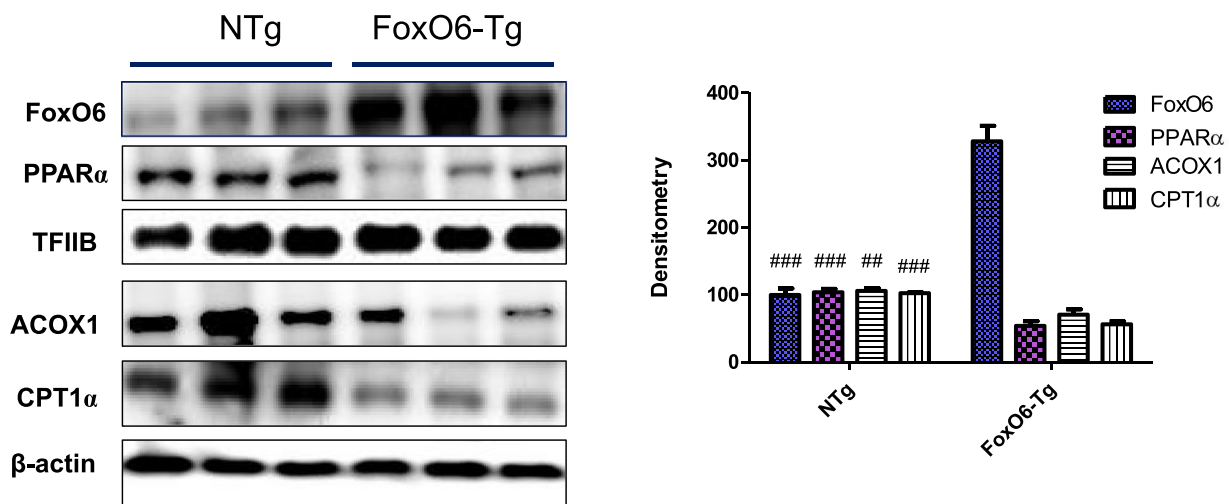
(B)
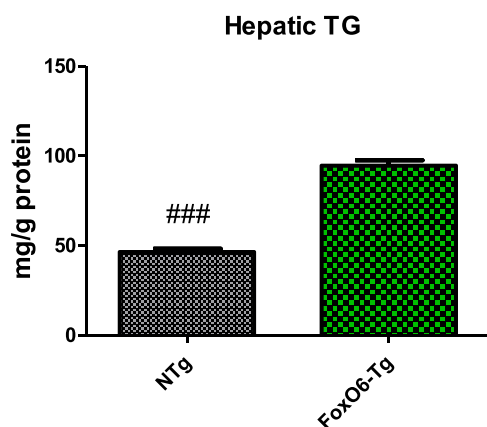
(C)

Fig. 6 FoxO6-induced lipid accumulation in the liver of FoxO6-Tg (each $n = 6$). **A** Western blot analysis of FoxO6, PPARα, ACOX1, and CPT1α in the nuclear and cytosol of FoxO6-Tg liver. TFIIB was the loading control of the nuclear fraction. β-actin was used as a loading control. Results of the one-factor ANOVA $^{\#\#}p < 0.01$ and $^{\#\#\#}p < 0.001$ vs. FoxO6-Tg. **B** Hepatic triglyceride levels in FoxO6-Tg. Results of the one-factor ANOVA $^{\#\#\#}p < 0.001$ vs. FoxO6-Tg. **C** The Western blot analysis showed that immunoprecipitated FoxO6 and PPARα were physically associated with PPARα and FoxO6 in FoxO6-Tg

Discussion

The major risk factor for the development of metabolic dysfunction–associated steatotic liver disease (MAFLD) [47] is excessive lipid accumulation in the liver by over-consumption of caloric intake, mainly owing to a high-fat diet [48]. Moreover, MAFLD is involved in metabolic disorders, including insulin resistance, dyslipidemia, and inflammation [49]. Previous research has determined that the expression of lipogenesis genes was increased in vivo and that this change was due to increased expression of the transcription factors FoxO1 and PPARγ, which are involved in lipid accumulation [50]. Our study characterized FoxO6 as a novel transcription factor that independently mediates hepatic lipogenesis during ER stress. We demonstrated crosstalk between FoxO6 and ER stress–induced hepatic lipogenesis. The lipotoxicity of MAFLD is caused by lipid oversupply directly influencing
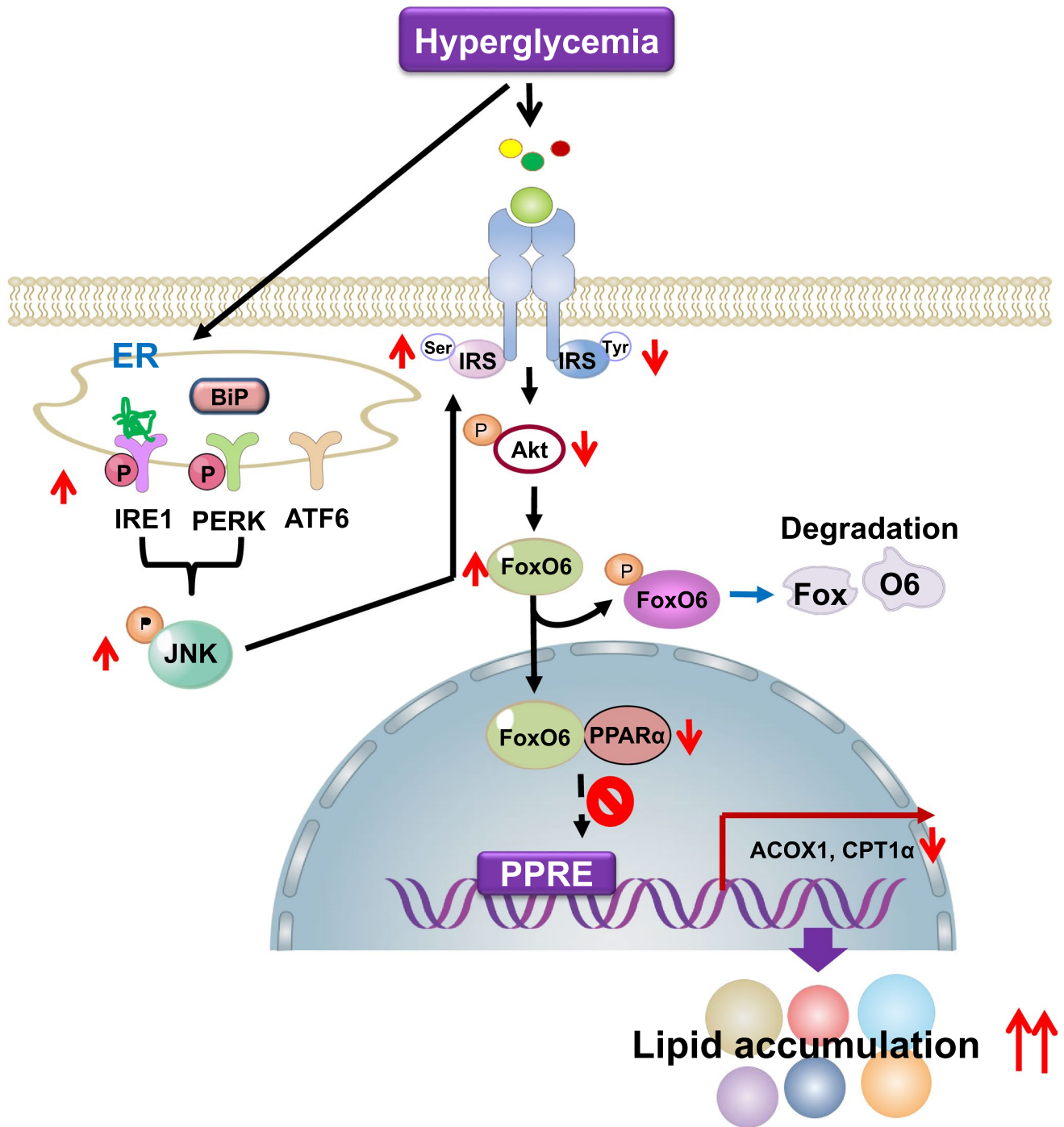
Fig. 7 Possible mechanism for how FoxO6 suppresses PPARα in lipogenesis

the balance between ER homeostasis and ER stress [51]. Thus far, little was known about FoxO6 and its regulatory role in ER stress–induced lipogenesis. When ER homeostasis is disturbed, unfolded proteins accumulate in the ER lumen, activating the UPR through dissociation of immunoglobulin protein/78 kDa glucose-regulated protein (BiP/GRP78) from PERK, IRE1α, and ATF6α [52, 53].

FoxO transcription factors are pivotal downstream targets of insulin/IGF-1 signaling and have been postulated to influence longevity by conferring increased resistance to oxidative stress, decreasing reactive oxygen species (ROS) production, and slowing the accumulation of oxidative damage [54, 55]. Some of these anti-oxidative effects are mediated by members of the FoxO family, which, in the

absence of insulin/IGF-1 signaling, bind to promoters of antioxidant enzymes and upregulate their expression [56]. These and other findings strongly suggest the involvement of FoxO in various diseases. For example, FoxO reduces the toxicity associated with aggregation-prone mutant proteins involved in human Alzheimer's and Huntington's disease, suggesting that the regulation of homeostasis during aging has a direct effect on the pathogeneses of human neurodegenerative diseases [57–59]. Additionally, FoxO6 was associated with elevated lipogenesis, contributing to increased fat accumulation in the liver of FoxO6-Tg mice (Supp. Figure 2). An increase in lipotoxicity will lead to insulin signaling. This study shows that ER stress can affect hepatic fat accumulation via FoxO6 activity.

FoxO6 involves inhibiter hepatic expression of the PPARα transcription factor. Our data further underscore the critical role of PPARα in promoting hepatic β-oxidation. In support of this notion, we showed that hepatic PPARα level significantly increased in response to FoxO6 knockout in the insulin-resistant liver, resulting in the downregulation of hepatic TG (Supp. Figure 3). However, FoxO6-CA significantly increased liver lipid accumulation and decreased the expression of PPARα and β-oxidation-associated genes (Fig. 2). These data also suggest that the FoxO6-mediated decrease in PPARα activity partially contributed to the increase in hepatic lipid accumulation. We found that liver lipid metabolism was severely impaired in the deficiency of PPARα with increased lipid accumulation (Fig. 3). To investigate the underlying mechanism, we showed that hepatic expression of CPT1α and ACOX1 genes were significantly downregulated, and the level of IRS/Akt protein decreased in the liver cells (Fig. 1). The strong association between hepatic steatosis and insulin resistance in human [60] and animal models [61, 62] suggests that insulin resistance may cause pathogenesis in obesity-related fatty liver disease.

In summary, the reciprocal activation ER stress attenuated insulin (IRS/Akt) signaling by a major mechanism underlying glucose-mediated hepatic lipogenesis and was caused by an altered interaction between FoxO6 and PPARα in vivo (Fig. 7). Our results provide significant insights into the cellular and molecular basis of the FoxO6/PPARα association. Accordingly, we propose this complex as a novel candidate target for the treatment of altered lipogenesis.

In conclusion, hyperglycemia-induced ER stress causes IRS/Akt inhibition, activating FoxO6 in vivo. Activation of FoxO6 interacts with PPARα, leading to hepatic steatosis in vivo and in vitro. Future research should focus on the potential application of these findings in the prevention of liver diseases and associated complications.

Supplementary Information The online version contains supplementary material available at https://doi.org/10.1007/s00109-024-02480-2.

Data availability All data generated or analyzed during this study are included in this published article.

Declarations

Ethical approval and consent to participate Not applicable.

Conflict of interest The authors declare no competing interests.

References

1. Jung UJ, Choi MS (2014) Obesity and its metabolic complications: the role of adipokines and the relationship betweenobesity, inflammation, insulin resistance, dyslipidemia and nonalcoholic fatty liver disease. Int J Mol Sci 15:6184–6223

2. Groneberg DA, Franke K, Klingelhöfer D, Schwarzer M, Ohlendorf D (2015) Density equalizing mapping of obesity: analysis of a global epidemic. Z Gastroenterol 53:553–561

3. Lin HV, Accili D (2011) Hormonal regulation of hepatic glucose production in health and disease. Cell Metab 14:9–19

4. Naidoo N (2009) ER and aging-protein folding and the ER stress response. Ageing Res Rev 8:150–159

5. Salminen A, Kaarniranta K (2010) ER stress and hormetic regulation of the aging process. Ageing Res Rev 9:211–217

6. Zhang W, Hietakangas V, Wee S, Lim SC, Gunaratne J, Cohen SM (2013) ER stress potentiates insulin resistance through PERK-mediated FOXO phosphorylation. Genes Dev 27:441–449

7. Salvado L, Palomer X, Barroso E, Vázquez-Carrera M (2015) Targeting endoplasmic reticulum stress in insulin resistance. Trends Endocrinol Metab 26:438–448

8. Accili D, Arden KC (2004) FoxOs at the crossroads of cellular metabolism, differentiation, and transformation. Cell 117:421–426

9. Barthel A, Schmoll D, Unterman TG (2005) FoxO proteins in insulin action and metabolism. Trends endocrinol Metabo 16:183–189

10. Biggs WH, Meisenhelder J, Hunter T, Cavenee WK, Arden KC (1999) Protein kinase B/Akt mediated phosphorylation promotes nuclear exclusion of the winged helix transcription factor FKHR1. Proc Natl Acad Sci USA 96:7421–7426

11. Kawamori D, Kaneto H, Nakatani Y, Matsuoka TA, Matsuhisa M, Hori M, Yamasaki Y (2006) The forkhead transcription factor Foxo1 bridges the JNK pathway and the transcription factor PDX-1 through its intracellular translocation. J Biol Chem 281:1091–1098

12. Urano F, Bertolotti A, Ron D (2000) IRE1 and efferent signaling from the endoplasmic reticulum. J Cell Sci 113:3697–3702

13. Ozcan U, Cao Q, Yilmaz E, Lee AH, Iwakoshi NN, Ozdelen E, Tuncman G, Görgün C, Glimcher LH, Hotamisligil GS (2004) Hotamisligil, Endoplasmic reticulum stress links obesity, insulin action, and type 2 diabetes. Science 306:457–461

14. Ozcan U, Yilmaz E, Ozcan L, Furuhashi M, Vaillancourt E, Smith RO, Görgün CZ, Hotamisligil GS (2006) Hotamisligil, Chemical chaperones reduce ER stress and restore glucose homeostasis in a mouse model of type 2 diabetes. Science 313:1137–1140

15. Lee AH, Glimcher LH (2009) Intersection of the unfolded protein response and hepatic lipid metabolism. Cell Mol Life Sci 66:2835–2850

16. Hotamisligil GS (2010) Endoplasmic reticulum stress and the inflammatory basis of metabolic disease. Cell 140:900–917

17. Lee AH, Scapa EF, Cohen DE, Glimcher LH (2008) Regulation of hepatic lipogenesis by the transcription factor XBP1. Science 320:1492–1496

18. Savage DB, Choi CS, Samuel VT, Liu ZX, Zhang D, Wang A, Zhang XM, Cline GW, Yu XX, Geisler JG, Bhanot S, Monia BP, Shulman GI (2006) Reversal of diet-induced hepatic steatosis and hepatic insulin resistance by antisense oligonucleotide inhibitors of acetyl-CoA carboxylases 1 and 2. J Clin Invest 116:817–824

19. Bánhegyi G, Baumeister P, Benedetti A, Dong D, Fu Y, Lee AS, Li J, Mao C, Margittai E, Ni M, Paschen W, Piccirella S, Senesi S, Sitia R, Wang M, Yang W (2007) Endoplasmic reticulum stress. Ann NY Acad Sci 1113:58–71

20. Oyadomari S, Mori M (2004) Roles of CHOP/GADD153 in endoplasmic reticulum stress. Cell Death Differ 11:381–389

21. Oh RS, Pan WC, Yalcin A, Zhang H, Guilarte TR, Hotamisligil GS, Christiani DC, Lu Q (2012) Functional RNA interference (RNAi) screen identifies system A neutral amino acid transporter 2 (SNAT2) as a mediator of arsenic-induced endoplasmic reticulum stress. J Biol Chem 287:6025–6034

22. Rosen ED, MacDougald OA (2006) Adipocyte differentiation from the inside out. Nat Rev Mol Cell Biol 7:885–896

23. Tontonoz P, Spiegelman BM (2008) Fat and beyond: the diverse biology of PPARγ. Annu Rev Biochem 77:289–312

24. Lehrke M, Lazar MA (2005) The many faces of PPARgamma. Cell 123:993–999

25. Matsusue K, Kusakabe T, Noguchi T, Takiguchi S, Suzuki T, Yamano S, Gonzalez FJ (2008) Hepatic steatosis in leptin-deficient mice is promoted by the PPARgamma target gene Fsp27. Cell Metab 7:302–311

26. Wierzbicki M, Chabowski A, Zendzian-Piotrowska M, Gorski J (2009) Differential effects of in vivo PPAR alpha and gamma activation on fatty acid transport proteins expression and lipid content in rat liver. J Physiol Pharmacol 60:99–106

27. Kim DH, Zhang T, Lee S, Calabuig-Navarro V, Yamauchi J, Piccirillo A, Fan Y, Uppala R, Goetzman E, Dong HH (2014) FoxO6 integrates insulin signaling with MTP for regulating VLDL production in the liver. Endocrinology 155:1255–1267

28. Zanetti M, Stocca A, Dapas B, Farra R, Uxa L, Bosutti A, Barazzoni R, Bossi F, Giansante C, Tedesco F, Cattin L, Guarnieri G, Grassi G (2008) Inhibitory effects of fenofibrate on apoptosis and cell proliferation in human endothelial cells in high glucose. J Mol Med 86:185–195

29. Clarke MCH, Figg N, Maguire JJ, Davenport AP, Goddard M, Littlewood TD, Bennett MR (2006) Apoptosis of vascular smooth muscle cells induces features of plaque vulnerability in atherosclerosis. Nat Med 12:1075–1080

30. Diep QN, Touyz RM, Schiffrin EL (2000) Docosahexaenoic acid, a peroxisome proliferator-activated receptor-alpha ligand, induces apoptosis in vascular smooth muscle cells by stimulation of p38 mitogen-activated protein kinase. Hypertension 36:851–855

31. Chen YC, Chu LY, Yang SF, Chen HL, Yet SF, Wu KK (2013) Prostacyclin and PPARα agonists control vascular smooth muscle cell apoptosis and phenotypic switch through distinct 14-3-3 isoforms. PLoS ONE 8:e69702

32. Kaur J (2014) A comprehensive review on metabolic syndrome. Cardiol Res Pract 943162:2014

33. Lefebvre P, Chinetti G, Fruchart JC, Staels B (2006) Sorting out the roles of PPAR alpha in energy metabolism and vascular homeostasis. J Clin Invest 116:571–580

34. Wang YX (2010) PPARs: Diverse regulators in energy metabolism and metabolic diseases. Cell Res 20:124–137

35. Hashimoto T, Cook WS, Qi C, Yeldandi AV, Reddy JK, Rao MS (2000) Defect in peroxisome proliferator-activated receptor alpha-inducible fatty acid oxidation determines the severity of hepatic steatosis in response to fasting. J Biol Chem 275:28918–28928

36. Xu J, Xiao G, Trujillo C, Chang V, Blanco L, Joseph SB, Bassilian S, Saad MF, Tontonoz P, Lee WNP, Kurland IJ (2002) Peroxisome proliferator-activated receptor alpha (PPARalpha) influences substrate utilization for hepatic glucose production. J Biol Chem 277:50237–50244

37. Fan CY, Pan J, Chu R, Lee D, Kluckman KD, Usuda N, Singh I, Yeldandi AV, Rao MS, Maeda N, Reddy JK (1996) Hepatocellular and hepatic peroxisomal alterations in mice with a disrupted peroxisomal fatty acyl-coenzyme A oxidase gene. J Biol Chem 271:24698–24710

38. Fan CY, Pan J, Usuda N, Yeldandi AV, Rao MS, Reddy JK (1998) Steatohepatitis, spontaneous peroxisome proliferation and liver tumors in mice lacking peroxisomal fatty acyl-CoA oxidase. Implications for peroxisome proliferator-activated receptor alpha natural ligand metabolism. J Biol Chem 273:15639–15645

39. Delerive P, Furman C, Teissier E, Fruchart J, Duriez P, Staels B (2000) Oxidized phospholipids activate PPARalpha in a phospholipase A2-dependent manner. FEBS Lett 471:34–38

40. Chakravarthy MV, Pan Z, Zhu Y, Tordjman K, Schneider JG, Coleman T, Turk J, Semenkovich CF (2005) "New" hepatic fat activates PPARalpha to maintain glucose, lipid, and cholesterol homeostasis. Cell Metab 1:309–322

41. Kim DH, Perdomo G, Zhang T, Slusher S, Lee S, Phillips BE, Fan Y, Giannoukakis N, Gramignoli R, Strom S, Ringquist S, Dong HH (2011) FoxO6 integrates insulin signaling with gluconeogenesis in the liver. Diabetes 60:2763–2774

42. Kamagate A, Qu S, Perdomo G, Su D, Kim DH, Slusher S, Meseck M, Dong HH (2008) FoxO1 mediates insulin-dependent regulation of hepatic VLDL production in mice. J Clin Invest 118:2347–2364

43. Altomonte J, Cong L, Harbaran S, Richter A, Xu J, Meseck M, Dong HH (2004) Foxo1 mediates insulin action on ApoC-III and triglyceride metabolism. J Clin Invest 114:1493–1503

44. Ables GP (2012) Update on PPARγ and nonalcoholic fatty liver disease. PPAR Res 2012:912351

45. Inoue M, Ohtake T, Motomura W, Takahashi N, Hosoki Y, Miyoshi S, Suzuki Y, Saito H, Kohgo Y, Okumura T (2005) Increased expression of PPARgamma in high fat diet-induced liver steatosis in mice. Biochem Biophys Res Commun 336:215–222

46. Calabuig-Navarro V, Yamauchi J, Lee S, Zhang T, Liu YZ, Sadlek K, Coudriet GM, Piganelli JD, Jiang CL, Miller R, Lowe M, Harashima H, Dong HH (2015) Forkhead Box O6 (FoxO6) Depletion attenuates hepatic gluconeogenesis and protects

against fat-induced glucose disorder in mice. J Biol Chem 290:15581–15594

47. Lazarus JV, Newsome PN, Francque SM, Kanwal F, Terrault NA, Rinella ME (2024) Reply: a multi-society Delphi consensus statement on new fatty liver disease nomenclature. Hepatology 79:E93–E94

48. Ip YT, Davis RJ (1998) Signal transduction by the c-Jun N-terminal kinase (JNK)–from inflammation to development. Curr Opin Cell Biol 10:205–219

49. Sheedfar F, Di Biase S, Koonen D, Vinciguerra M (2013) Liver diseases and aging: friends or foes? Aging Cell 12:950–954

50. Kim DH, Ha S, Choi YJ, Dong HH, Yu BP, Chung HY (2019) Altered FoxO1 and PPARγ interaction in age-related ER stress-induced hepatic steatosis. Aging-US 11:4125–4144

51. Leamy AK, Egnatchik RA, Young JD (2013) Molecular mechanisms and the role of saturated fatty acids in the progression of non-alcoholic fatty liver disease. Prog Lipid Res 52:165–174

52. Walter P, Ron D (2011) The unfolded protein response: from stress pathway to homeostatic regulation. Science 334:1081–1086

53. Wang S, Kaufman RJ (2012) The impact of the unfolded protein response on human disease. J Cell Biol 197:857–867

54. Balaban R, Nemoto S, Finkel T (2005) Mitochondria, oxidants, and aging. Cell 120:483–495

55. Panici JA, Harper JM, Miller RA, Bartke A, Spong A, Masternak MM (2010) Early life growth hormone treatment shortens longevity and decreases cellular stress resistance in long-lived mutant mice. FASEB J 24:5073–5079

56. Kops GJ, Dansn TB, Polderman PE, Saarloos I, Wirtz KW, Coffer PJ, Huang TT, Bos JL, Medema RH, Burgering BM (2002) Forkhead transcription factor FOXO3a protects quiescent cells from oxidative stress. Nature 419:316–321

57. Cohen E, Bieschke J, Perciavalle RM, Kelly JW, Dillin A (2006) Opposing activities protect against age-onset proteotoxicity. Science 313:1604–1610

58. Hsu AL, Murphy CT, Kenyon C (2003) Regulation of aging and age-related disease by DAF-16 and heat-shock factor. Science 300:1142–1145

59. Morley JF, Brignull HR, Weyers JJ, Morimoto RI (2002) The threshold for polyglutamine-expansion protein aggregation and cellular toxicity is dynamic and influenced by aging in Caenorhabditis elegans. Proc Natl Acad Sci USA 99:10417–10422

60. Marceau P, Biron S, Hould FS, Marceau S, Simard S, Thung SN, Kral JG (1999) Liver pathology and the metabolic syndrome X in severe obesity. J Clin Endocrinol Metab 84:1513–1517

61. Uysal KT, Wiesbrock SM, Marino MW, Hotamisligil GS (1997) Protection from obesity-induced insulin resistance in mice lacking TNF-alpha function. Nature 389:610–614

62. Shimomura I, Bashmakov Y, Horton JD (1999) Increased levels of nuclear SREBP-1c associated with fatty livers in two mouse models of diabetes mellitus. J Biol Chem 274:30028–30032